


Complex formation of cetirizine drug with bivalent transition metal(II) ions in the presence of alanine: synthesis, characterization, equilibrium studies, and biological activity studies

Ahmed M. Rayan, Mahmoud M. Ahmed, Mohamed H. Barakat, Abeer T. Abdelkarim & Ahmed A. El-Sherif

To cite this article: Ahmed M. Rayan, Mahmoud M. Ahmed, Mohamed H. Barakat, Abeer T. Abdelkarim & Ahmed A. El-Sherif (2015) Complex formation of cetirizine drug with bivalent transition metal(II) ions in the presence of alanine: synthesis, characterization, equilibrium studies, and biological activity studies, Journal of Coordination Chemistry, 68:4, 678-703, DOI: [10.1080/00958972.2014.994513](https://doi.org/10.1080/00958972.2014.994513)

To link to this article: <http://dx.doi.org/10.1080/00958972.2014.994513>

 View supplementary material [↗](#)

 Accepted author version posted online: 03 Dec 2014.
Published online: 09 Jan 2015.

 Submit your article to this journal [↗](#)

 Article views: 73

 View related articles [↗](#)

 View Crossmark data [↗](#)

 Citing articles: 2 View citing articles [↗](#)

Complex formation of cetirizine drug with bivalent transition metal(II) ions in the presence of alanine: synthesis, characterization, equilibrium studies, and biological activity studies

AHMED M. RAYAN*^{†‡}, MAHMOUD M. AHMED[‡], MOHAMED H. BARAKAT[§],
ABEER T. ABDELKARIM[¶] and AHMED A. EL-SHERIF^{†¶}

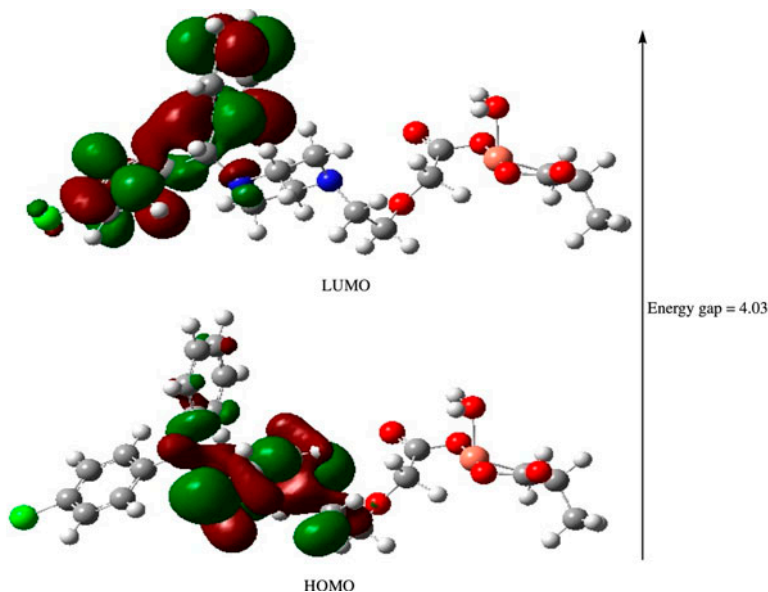
[†]Faculty of Arts and Science, Department of Chemistry, Northern Border University, Rafha, KSA

[‡]New-Valley Faculty of Education, Department of Sciences and Mathematics, Assiut University, Assiut, Egypt

[§]Holding Company for Water and Waste Water, The Reference Laboratory for Drinking Water, Inorganic Laboratory, Cairo, Egypt

[¶]Faculty of Science, Department of Chemistry, Cairo University, Cairo, Egypt

(Received 26 May 2014; accepted 10 November 2014)



The present article reports on the synthesis, characterization, and their electronic absorption spectra of M(II)–ternary complexes involving CTZ as antihistamine drug and alanine as a representative example of amino acids. The geometry of the studied M(II) complexes has been fully optimized

*Corresponding author. Email: amtrayan@yahoo.com

using parameterized PM3 semi-empirical method. Protonation and complex formation equilibria were investigated. The antimicrobial activities were investigated.

Mononuclear cobalt(II), nickel(II), and copper(II) complexes of cetirizine·2HCl (CTZ = 2-[2-[4-[(4-chlorophenyl)phenyl methyl]piperazine-1-yl]-ethoxy]acetic acid) in the presence of alanine (Ala) as a representative example of amino acids were synthesized and elucidated by different physical techniques. All complexes have been characterized with the help of elemental analyses, molecular weights, molar conductance values, magnetic moments, and spectroscopic data. The measured molar conductance values in DMSO indicate that the complexes are nonelectrolytes. Quantum chemical calculations were performed with semi-empirical method to find the optimum geometry of complexes. The metal–oxygen bond length in the synthesized complexes obeys the order $M-OH_2 > M-O_{CTZ} > M-O_{Ala}$. Formation equilibria of the ternary complexes have been investigated. Ternary complexes are formed by a simultaneous mechanism. Stoichiometry and stability constants for the complexes formed are reported. The concentration distributions of various species formed in solution were also evaluated as a function of pH. CTZ and its metal chelates have been screened for their antimicrobial activities against some selected types of gram-positive (G^+) and gram-negative (G^-) bacteria. They were more active against (G^+) than (G^-) bacteria.

Keywords: Cetirizine; Potentiometry; Alanine; Molecular modeling; Spectra; Biological activity

1. Introduction

Metal chelation is involved in many important biological processes where the coordination can occur between a variety of the metal ions and a wide range of ligands [1, 2]. Complexes derived from potent bioactive ligands containing N,O donor binding sites with M(II) ions are used in biological, analytical, agricultural, industrial, and therapeutic applications [3, 4]. Metal ions are fundamental elements for healthy life to humans and higher animals [5], particularly the late first-row transition metals such as cobalt, nickel, copper, and zinc are biologically relevant metals associated with various biomolecules related to essential physiological activities. Copper is a crucial trace element for many biological functions [6]. Cu(II) plays a vital role for the development of connective tissue, nerve coverings, and bone in humans. Copper with its bioessential activity and oxidative nature has attracted numerous inorganic chemists to address Cu(II) complexes for various biological activities, including antibacterial [7, 8], antitumor [8–10], antifungal [11, 12], antioxidant [13], and antiinflammatory [14]. Cobalt is an essential trace element in animal nutrition and in the form of vitamin B₁₂, essential for human health as it stimulates the production of red blood cells. Cobalt associates with important synthetic reactions in the metabolic process [15]. Nickel is also essential, associated with several enzymes and playing a role in physiological processes as a cofactor in the absorption of iron from the intestine [16]. Any change in its concentration leads to metabolic disorder [17]. With the biological importance of copper, cobalt, and nickel, it is important to study complexation with bioactive ligands to understand functions of their complexes and to find new bioactive compounds.

Amino acids are the basic components of living organisms and constitute the building blocks of proteins found in structural tissues of the human body. Amino acids are the chemical units of proteins [18] and essential for various biochemical processes that support life in individuals [19, 20]. They are good chelating agents [21] and can coordinate to transition metals through their amino or carboxylic groups [22, 23]. Complexation of transition metal ions with amino acids have been studied [24–26]. The amino acid–metal ion interactions are responsible for enzymatic activity and stability of protein structures [27–29]. Study of thermodynamic parameters will help to investigate the driving forces that lead to formation of metal–amino acid complexes in biological systems. Also, amino acids and their

mixed-ligand complexes are employed in biology, pharmacy, industry, and laboratory reagents [30]. Furthermore, ternary complexes formed between metal ions and two different bioligands, such as heteroaromatic nitrogen bases and amino acids, may be considered as models for substrate–metal ion–enzyme interactions and other metal ion-mediated biochemical interactions [31].

In continuation of our interest in studying coordination behavior of biologically active compounds [10–14, 32–39], we report here synthesis of systems including Co(II), Ni(II), Cu(II), CTZ, and alanine (Ala) as a representative example of amino acids and characterization of these chelates using elemental analyses, IR, ESR, UV–vis, magnetic moment, and molar conductance. Metal chelates have been screened for their antibacterial and antifungal activities. We also identify all complexes which form in aqueous solution and the driving forces for their formation on the basis of derived equilibria and stability constants. Thus, in the present study, together with study of the ternary systems in the solid state, a systematic study of complex formation between some essential bivalent metal ions, CTZ and Ala (scheme 1) was carried out using a potentiometric titration technique at $I = 0.20 \text{ M dm}^{-3}$ (NaCl) at different temperatures to determine the protonation and stability constants of the formed complexes.

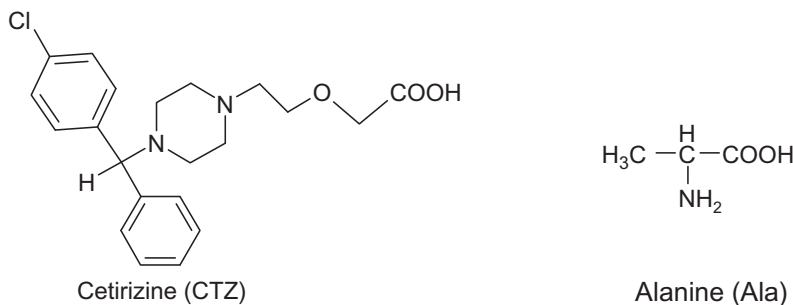
2. Experimental

2.1. Materials and reagents

Cetirizine, $\text{CoCl}_2 \cdot 6\text{H}_2\text{O}$, $\text{NiCl}_2 \cdot 6\text{H}_2\text{O}$, $\text{CuCl}_2 \cdot 2\text{H}_2\text{O}$, and α -alanine were provided by Sigma Chemical Co. Carbonate-free NaOH solutions (titrant) were prepared by diluting BDH (British Drug House)-concentrated volumetric solution vials. These solutions were systematically checked by titration against potassium hydrogen phthalate solution. All solutions were prepared in deionized H_2O .

2.2. Preparation of the solid complexes

The 1 : 1 : 1 [M : CTZ : Ala] complexes were prepared from hot ethanolic solutions (90°C) by the addition of 25 mL of metal chloride (1 mM, 2.38 g $\text{CoCl}_2 \cdot 6\text{H}_2\text{O}$, 2.37 g $\text{NiCl}_2 \cdot 6\text{H}_2\text{O}$, 0.170 g $\text{CuCl}_2 \cdot 2\text{H}_2\text{O}$) dropwise to 25 mL of CTZ (1 mM, 0.4618 g) and Ala (1 mM, 0.89 g). An equivalent amount of NaHCO_3 was added to neutralize the released protons. The obtained mixture was refluxed with stirring for 5–6 h and then kept in the



Scheme 1. Structural formulas of cetirizine and alanine amino acid.

refrigerator overnight. Thus, the formed complexes were filtered, collected, and then washed several times with ethanol and then diethyl ether. The solid complexes were dried in a vacuum desiccator. The yield ranged from 65 to 77%. The complexes are soluble in DMF and DMSO. The dried complexes were subjected to elemental and spectroscopic analysis.

2.3. Molecular modeling

An attempt to gain better insight on the molecular structure of these synthesized compounds, geometric optimization, and conformation analysis was performed using semiempirical parameterized PM3 method as implemented in HyperChem 7.5 [40]. A gradient of 1×10^{-2} cal $\text{\AA}^{-1} \text{M}^{-1}$ was set as a convergence criterion in all the quantum calculations.

2.4. Biological activity

Antimicrobial activity of the tested samples was determined using a modified Kirby-Bauer disk diffusion method [41] as reported using standard disks of *Gentamicin* and *Ampicillin* for G^- (*Escherichia coli* RCMB010052 and *Pseudomonas aeruginosa* RCMB010043) and G^+ (*Staphylococcus aureus* RCMB010028 and *Bacillus subtilis* RCMB010067) bacterial species, and *Amphotericin B* for antifungal activity versus four filamentous fungi (*Aspergillus flavus* RCMB 02568, *Penicillium italicum* RCMB 03924, *Candida albicans* RCMB 05031, *Geotricum candidum* RCMB 05097). Biological activity studies were carried out as reported in [41–45].

2.5. Instruments

Potentiometric measurements were made using a Metrohm 686 titroprocessor equipped with a 665 Dosimat (Switzerland-Herisau). A thermostatted glass-cell equipped with a magnetic stirring system, a Metrohm glass electrode, a thermometric probe, a microburet delivery tube, and a salt bridge connected with the reference cell filled with 0.1 M KCl solution in which saturated calomel electrode was dipped was used. Temperature was maintained constant inside the cell at 25.0 ± 0.02 °C, by the circulating water of a thermostated bath (precision ± 0.02). The titroprocessor and electrode were calibrated with standard buffer solutions, potassium hydrogen phthalate (pH 4.008), and a mixture of KH_2PO_4 and Na_2HPO_4 (pH 6.865) at 25.0 °C. The microchemical analysis of the separated solid chelates for C, H, and N were performed in the Microanalytical Center, Cairo University. The analyses were performed twice to check the accuracy of the analysis data. Infrared spectra were recorded on an 8001-PC FTIR Shimadzu spectrophotometer using KBr pellets. Solid reflectance spectra were measured on a Shimadzu 3101 pc spectrophotometer. The molar conductances of the complexes were measured for 1.00×10^{-3} M DMSO solutions at 25 ± 1 °C using a systronic conductivity bridge type 305. The room temperature magnetic susceptibility measurements for the complexes were determined by a Gouy balance using $\text{Hg}[\text{Co}(\text{SCN})_4]$ as a calibrant. A Shimadzu TGA-50H thermal analyzer was used to record simultaneously TG and DTG curves at the Micro Analytical Center, Cairo University, Cairo, Egypt. All experiments were performed using a single loose top loading platinum sample pan under nitrogen at a flow rate of 10 mL min^{-1} .

2.6. Procedures and measurements

The following mixtures were prepared and titrated potentiometrically with 0.05 M NaOH solution: (A) 40 mL of solution containing $1.25 \times 10^{-3} \text{ M dm}^{-3}$ M(II) and 0.1 M dm^{-3} NaCl; (B) 40 mL of solution containing $1.25 \times 10^{-3} \text{ M dm}^{-3}$ ligand (CTZ or Ala) of constant ionic strength 0.1 M dm^{-3} (adjusted with NaCl); (C) 40 mL of solution containing $1.25 \times 10^{-3} \text{ M dm}^{-3}$ Co^{II}/Ni^{II}, or Cu^{II}, $2.5 \times 10^{-3} \text{ M dm}^{-3}$ ligand (CTZ or Ala), and 0.1 M dm^{-3} NaCl; and (D) 40 mL of solution containing $1.25 \times 10^{-3} \text{ M dm}^{-3}$ Co^{II}/Ni^{II}, or Cu^{II} ion, $1.25 \times 10^{-3} \text{ M dm}^{-3}$ CTZ, and $1.25 \times 10^{-3} \text{ M dm}^{-3}$ Ala at 0.1 M dm^{-3} NaCl.

The hydrolysis constants of M^{II} were determined by titrating mixture A. The proton association constants of the ligands were determined potentiometrically by titrating mixture B. The stability constants of the binary M(II)–CTZ and M–Ala complexes were determined by titrating mixture C. The stability constants of the mixed-ligand complexes were determined using potentiometric data obtained from mixture D. All titrations were performed in a purified N₂ atmosphere using aqueous 0.05 M dm^{-3} NaOH as titrant.

The pH meter readings were converted into hydrogen ion concentration by titrating a standard acid solution (0.05 M dm^{-3}) with standard base solution (0.05 M dm^{-3}) at 25 °C and $I = 0.1 \text{ M dm}^{-3}$ NaNO₃. The pH is plotted against p[H]. The relationship pH–p[H] = 0.05 was observed; [OH[–]] value was calculated using a pK_w value of 13.921 [46].

The general four-component equilibrium can be written as follows: (charges are omitted for simplicity).



$$\beta_{1pqr} = \frac{[\text{M}_1(\text{CTZ}_p)(\text{AA}_q)(\text{H}_r)]}{\text{M}^1(\text{CTZ}^p)(\text{AA}^q)(\text{H}^r)} \quad (2)$$

2.7. Data processing

The calculations were obtained from ca. 100 data points in each titration using the computer program MINQUAD-75 [47]. The species distribution diagrams were obtained using the program SPECIES [48] under the experimental condition employed. All measurements were carried out in our laboratory at Cairo University.

Table 1. Analytical and physical data of compounds.

Complex	Mwt	% Yield	m/z	% C		% H		% N		% Cl	
				Calcd	Found	Calcd	Found	Calcd	Found	Calcd	Found
[Cu(CTZ)(Ala)(H ₂ O)] (1)	557.5	77	558	51.70	51.75	5.78	5.82	7.53	7.55	6.36	6.38
[Ni(CTZ)(Ala)(H ₂ O)] (2)	552.6	72	553	52.16	52.19	5.83	5.89	7.60	7.65	6.41	6.44
[Co(CTZ)(Ala)(H ₂ O)]·H ₂ O (3)	570.9	65	571	52.13	52.21	5.83	5.87	7.59	7.62	6.42	6.48

3. Results and discussion

All compounds are stable in air. The interaction of CTZ and alanine with metal(II) salts in EtOH in a molar ratio 1 : 1 : 1 under reflux conditions in the presence of an equivalent amount of NaHCO₃ to neutralize the released protons gave the metal complexes presented in table 1. The formulation of these complexes is based on elemental analysis, IR, EPR, UV-vis, and electrical conductivity. The complexes are insoluble in H₂O and other common organic solvents, but soluble in DMF and DMSO.

3.1. IR Spectra and mode of bonding

The results of IR measurements are listed in table 2 with assignments for most of the major peaks for the free ligands and their metal(II) complexes. IR spectra of CTZ reveal the appearance of characteristic absorptions at 3470, 2375, 1740, and 1186 cm⁻¹, which can be attributed to stretching frequencies of νOH, quaternary N stretch in hydrochloride, νCO_{carb}-boxylic, and νC-Oaliphatic, respectively. The aliphatic chain C-O bond in CH₂CH₂OCH₂- appears at 1186 cm⁻¹. As expected, this band is not affected by chelation. In IR spectra, disappearance of the OH band at 3470 cm⁻¹, characteristic of carboxylic acid, confirms the deprotonation and complexation. The IR spectrum of CTZ also shows a band at 1740 cm⁻¹ corresponding to ν(C=O)_{carb}. The peak at 1740 cm⁻¹ corresponding to ν(C=O)_{carb} of CTZ disappears on complexation with metal ion, replaced by ν(COO)_{as} = ~1609–1631 cm⁻¹ and ν(COO)_s = ~1406–1412 cm⁻¹ [49]. Decon showed that the magnitude of Δν [Δν = ν_{asy}(COO⁻) - ν_{sym}(COO⁻)] can be correlated with the coordination modes of the carboxylate [50–52]. This difference is >200 cm⁻¹ reflecting monodentate coordination of carboxylate of CTZ in the complexes. Far IR spectra of complexes reveal ν(M-O) stretching vibrations at 485–494 cm⁻¹. For Ala, bands at 1605 and 1413 cm⁻¹ due to ν_{asym}(COO⁻) and ν_{sym}(COO⁻) appear in the complexes at 1500–1514 and 1295–1309 cm⁻¹, respectively. Monodentate carboxylate of alanine is proved by frequency separation of ~201–214 cm⁻¹ (Δν = νCOO_{as} - νCOO_s) [53, 54]. The shift of these two bands suggests involvement of the carboxylic group of the amino acids in complex formation. The Δ_{NH3+} band, which is characteristic of the zwitter ion, disappears in spectra of the complexes, i.e. Δ_{NH3+} of free alanine at 1623 cm⁻¹ disappears on coordination, indicating that the NH₂ group is deprotonated and binds to the metal ion through the neutral amino group. Hence, the amino acid is chelated to the metal ion through a five-membered chelate ring. The presence of

Table 2. Tentative assignment of the important infrared bands of the complexes.

Compound	ν (cm ⁻¹)							
	ν _{H₂O}	Cetirizine ν _{C=O}	Alanine			Far IR		
			Δ _{NH3+} (Free AA)	ν _{asym} (COO)	ν _{sym} (COO)	ν _(M-O) (CTZ)	ν _(M-N) (AA)	ν _(M-O) (AA)
CTZ	–	1740	–	–	–	–	–	–
Ala	–	–	1623	1597	1412	–	–	–
1	3430, 810, 760	1621, 1406	Disapp.	1510	1309	490	430	510
2	3450, 802, 750	1631, 1419	Disapp.	1514	1300	485	410	535
3	3420, 812, 760	1610, 1407	Disapp.	1500	1295	494	412	520

α-Ala = α-Alanine and CTZ = 2-[2-[4-[(4-chlorophenyl)phenyl methyl]piperazine-1-yl]-ethoxy]acetic acid.

water in the compounds is deduced from the elemental analysis and IR spectrum. The strong and broad peaks centered at 3420–3450 cm^{-1} represent the O–H stretch of coordinated and/or hydrated water [55, 56]. The presence of coordinated water in these complexes has been inferred on the basis of a medium intensity band at 750–760 cm^{-1} and 802–812 cm^{-1} assignable to the OH rocking and wagging vibrations, respectively [10, 54, 57]. The far IR spectra of complexes reveal that $\nu(\text{M–N})$ and $\nu(\text{M–O})$ stretches are 410–430 and 510–535 cm^{-1} , respectively. Thus, it is evident that Ala is bonded bidentate to the metal through the amino and carboxylate groups. CTZ is coordinated monodentate to the metal through carboxylate.

3.2. Molar conductance measurements

Using the relation $\Lambda_{\text{M}} = \text{K}/\text{C}$, the molar conductance values of the prepared complexes at 1×10^{-3} M in DMSO solution are 3.2–5.5 $\Omega^{-1} \text{cm}^2 \text{M}^{-1}$ as given in table 3. These low values indicated that all synthesized complexes are nonelectrolytes [58, 59]. Conductivity measurements are in agreement with the elemental analysis data.

3.3. Electronic, mass spectra, and magnetic measurements

Solid reflectance spectra and magnetic moment measurements are used for elucidation of M(II) complexes. The solid state spectra of Cu(II) compound exhibits a d–d band transition at 15,360 cm^{-1} , which is consistent with a broad structured band for square-planar complexes in the range 600–700 cm^{-1} . In the present study, the broad band for $[\text{Cu}(\text{CTZ})(\text{Ala})(\text{H}_2\text{O})]$ (figure 1S, see online supplemental material at <http://dx.doi.org/10.1080/00958972.2014.994513>) is due to ${}^2\text{B}_{1\text{g}} \rightarrow {}^2\text{A}_{1\text{g}}$ as reported for square-planar Cu(II) complexes [60, 61]. The band observed at 26,667 cm^{-1} was tentatively assigned to a ligand to metal charge transition (MLCT). The absence of bands below 10,000 cm^{-1} eliminates the possibility of a tetrahedral or octahedral environment for this copper(II) center [60, 62]. The magnetic moment of the copper(II) complex corresponds to μ_{eff} value for one unpaired electron (1.93 BM) [53, 63, 64]. X-band ESR spectra of Cu(II) complex was recorded in the solid state at room temperature. The spectrum exhibits one broad band with $g = 2.05$ (figure 2S). The shape of the spectrum is consistent with the square-planar geometry around Cu(II).

The electronic spectrum of the Ni(II) complex (2) shows a band at 17,544 cm^{-1} assigned to the ${}^1\text{A}_{1\text{g}} \rightarrow {}^1\text{A}_{2\text{g}}$ transition [64, 65]. The supplementary band at 26,250 cm^{-1} was tentatively assigned to a ligand to metal charge transition. The assumed square-planar geometry

Table 3. Molar conductance, magnetic moment, electron paramagnetic resonance, and electronic spectral data of $\text{M}^{\text{II}}\text{–CTZ–Ala}$ complexes.

Complex	$\Lambda_{\text{M}}^{\text{a}}$	μ_{eff} (BM)	λ_{max} (cm^{-1})	Assignment	Geometry
$[\text{Cu}(\text{CTZ})(\text{Ala})(\text{H}_2\text{O})]$ (1)	2.6	1.93	15,360 26,667	${}^2\text{B}_{1\text{g}} \rightarrow {}^2\text{A}_{1\text{g}}$ CT	Square planar
$[\text{Ni}(\text{CTZ})(\text{Ala})(\text{H}_2\text{O})]$ (2)	3.2	0	17,544 26,250	${}^1\text{A}_{1\text{g}} \rightarrow {}^1\text{A}_{2\text{g}}$ CT	Square planar
$[\text{Co}(\text{CTZ})(\text{Ala})(\text{H}_2\text{O})] \cdot \text{H}_2\text{O}$ (3)	4.4	2.77	17,007 20,833 29,154	${}^2\text{A}_{1\text{g}} \rightarrow {}^2\text{B}_{2\text{g}}$ ${}^2\text{A}_{1\text{g}} \rightarrow {}^2\text{E}_{\text{g}}$ CT	Square planar

^aMolar conductance measured for 10^{-3} M DMSO solution, $\Omega^{-1} \text{cm}^2 \text{M}^{-1}$.

for this complex is confirmed from the value of its room temperature magnetic moment of zero.

The electronic spectrum of the Co(II) complex (**3**) (figure 3S) showed bands at 17,007 and 20,833 cm^{-1} which may be assigned to ${}^2A_{1g} \rightarrow {}^2B_{2g}$ and ${}^2A_{1g} \rightarrow {}^2E_g$ transitions, respectively, for Co(II) in a square-planar geometry [66]. The band observed at 29,154 cm^{-1} was tentatively assigned to MLCT. The room temperature magnetic moment of [Co(CTZ)(Ala)(H₂O)] of 2.77 BM is more than that of low spin octahedral and lower than the values characteristic of tetrahedral cobalt(II) complexes (4.2–4.7 BM). Furthermore, this value is similar to that reported for the square-planar cobalt(II) complexes [67–69].

The mass spectrum of the nickel(II) complex as a representative example of M(II) complexes (figure 1) showed the first mass peak at m/e 553 which agrees well with the molecular ion peak for [Ni(CTZ)(Ala)(H₂O)] complex, confirming its structure.

3.4. Thermal analysis

Thermal gravimetric analysis (TGA) was used to determine associated water or solvent molecules in the coordination sphere or in the outer sphere of the complex. Results of thermal studies of the complexes are concordant with their formulation. In the present investigation, the heating rates were 10 $^{\circ}\text{C}/\text{min}$ under nitrogen and the weight loss was measured from room temperature to $\cong 850$ $^{\circ}\text{C}$. The correlations between the different decomposition steps of the complexes with the corresponding weight losses are discussed in terms of the proposed formulas of the complexes. The results of thermal analyses showed agreement with the formula as suggested from the elemental analyses. The suggested intermediates and final products are given in table 4. The thermal curves (TG and DTG) of all the complexes are similar and show that decomposition takes place in three steps except Co(II) complex occurs in four steps due to water of hydration in this complex eliminated in a separate step. The decomposition of all complexes ended with metal oxide residue. A schematic representation of [Cu(CTZ)(Ala)(H₂O)] (**1**) as a representative example of metal(II)–mixed-ligand complexes is shown in scheme 2. **1** was stable to 130 $^{\circ}\text{C}$. Above this temperature, coordinated water molecule is eliminated in one step at 130–205 $^{\circ}\text{C}$ with a mass loss of 3.51% (Calcd 3.23%). The second step from 330 to 450 $^{\circ}\text{C}$ was assigned to removal of CTZ with mass loss of 69.37% (Calcd 69.57%). The third step with mass loss of 12.93% at 610–705 $^{\circ}\text{C}$ was assigned to removal of alanine leaving CuO as residue.

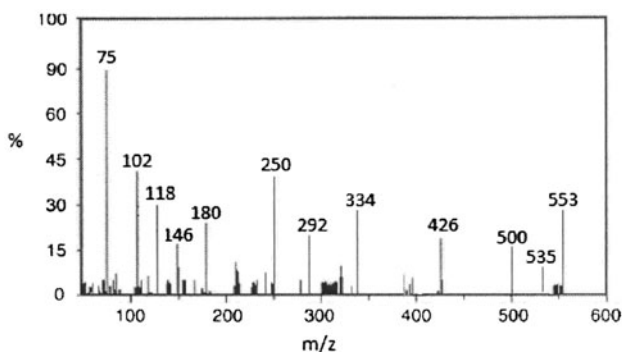


Figure 1. Mass spectrum of [Ni(CTZ)(Ala)(H₂O)].

Table 4. TGA data for the investigated metal(II) complexes.

Complex	T (°C)	Weight loss		Assignment	Metallic residue
		% Found	% Calcd		
[Cu(CTZ)(Ala)(H ₂ O)]	130–205	3.51	3.23	Elimination of coordinated H ₂ O	CuO
	330–450	69.37	69.57	Elimination of CTZ	(% Found 14.15, % Calcd 14.27)
	610–705	12.77	12.93	Elimination of C ₃ H ₆ ON	
[Ni(CTZ)(Ala)(H ₂ O)]	145–211	3.15	3.26	Elimination of coordinated H ₂ O	NiO
	319–467	70.23	70.19	Elimination of CTZ	(% Found 13.10 % Calcd 13.51)
[Co(CTZ)(Ala)(H ₂ O)]·H ₂ O	688–790	13.14	13.04	Elimination of C ₃ H ₆ ON	
	30–90	3.19	3.15	Elimination of hydrated H ₂ O	CoO
	122–194	3.28	3.15	Elimination of coordinated H ₂ O	(% Found 13.32 % Calcd 13.12)
	340–470	67.23	67.93	Elimination of CTZ	
	622–758	12.71	12.62	Elimination of C ₃ H ₆ ON	

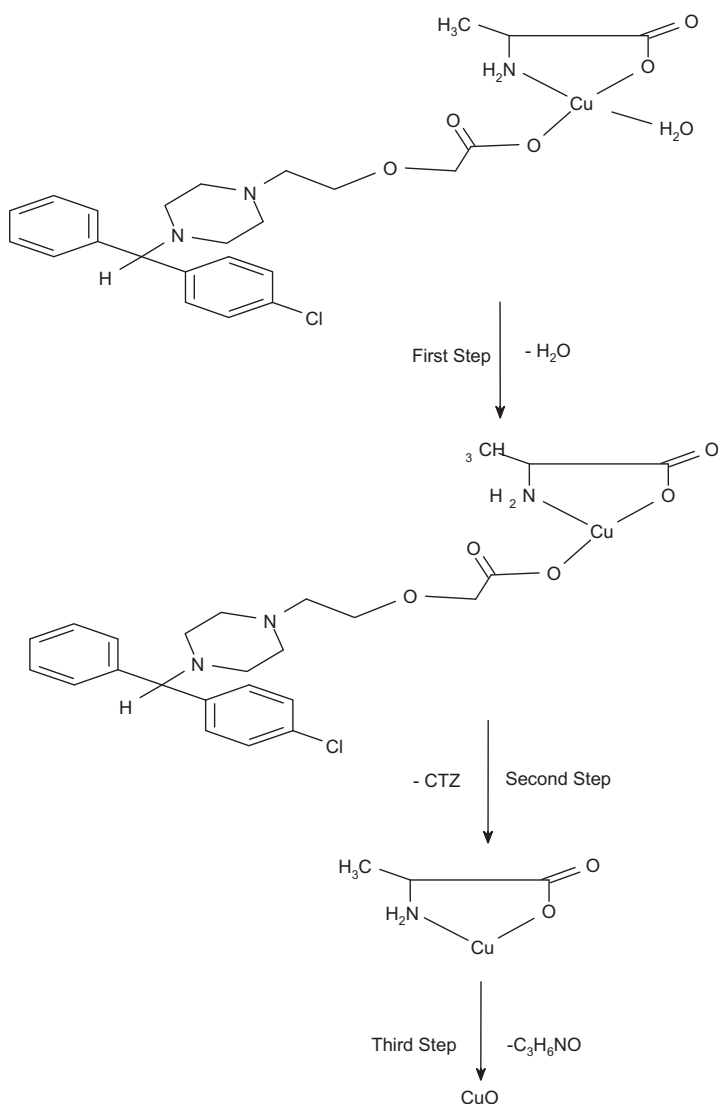
[Ni(CTZ)(Ala)(H₂O)] (**2**) (figure 4S) was stable to 118 °C, where coordinated water is eliminated in one step with a mass loss of 3.15% (Calcd 3.26%). The second step at 319–467 °C was assigned to removal of CTZ with mass loss of 70.23% (Calcd 70.19%). The third step from 688 to 790 °C with mass loss of 13.14% (Calcd 13.04%) at 703–790 °C was assigned to removal of alanine leaving NiO as residue.

The TGA curve of [Co(CTZ)(Ala)(H₂O)]·H₂O shows four stages of decomposition. The first at 30–90 °C corresponds to loss of water of hydration with mass loss of 3.19% (Calcd 3.15%). The second step of decomposition from 122 to 194 °C corresponds to loss of water of coordination with mass loss of 3.28% (Calcd 3.15%). The third step (340–470 °C) corresponds to CTZ loss (mass loss 67.23%; Calcd 67.93%). The fourth step (622–758 °C) corresponds to elimination of Ala (loss of C₃H₆NO moiety) with mass loss of 12.71% (Calcd 12.62%). The total mass loss to 758 °C is in agreement with the formation of CoO as the final residue (TG 13.32%; Calcd 13.12%).

3.5. Molecular modeling

Energy minimization studies were carried out on the basis of the semi-empirical PM3 level provided by HyperChem 7.5 software. The molecular parameters were calculated after geometrical optimization of the structures of M(II) complexes (table 5). The molecular structure of Cu(II) complex along with the atom numbering scheme is given in figure 2.

3.5.1. Geometry optimization. Geometry optimization was done using the semi-empirical PM3 level incorporated in the HyperChem 7.5 program in the gas phase. The copper(II) bond lengths and angles are given in table 1S. Selected bond lengths and angles of metal (II) complexes are given in table 6. Metal(II) complexes have square-planar geometry. The equatorial positions of square-planar geometry are occupied by nitrogen and oxygen of Ala, oxygen of carboxylate of CTZ, and oxygen of water. From analysis of the data in table 6 for the bond lengths and angles, one can conclude the following: (1) The angles around the metal undergo appreciable variations upon changing the metal center; (2) The M–N_{Ala} bond distances [1.914(1), 1.844(2), and 1.905(3) Å], the M–O_{CTZ} bond distances [1.888(1), 1.842(2), and 1.909(3) Å], the M–O_{Ala} bond distances [1.873(1), 1.830(2), and 1.878(3) Å],



Scheme 2. The thermogravimetric decomposition pattern of $[\text{Cu}(\text{CTZ})(\text{Ala})(\text{H}_2\text{O})]$.

and the $\text{M}-\text{O}_{\text{water}}$ bond distances [1.961(1), 1.893(2), and 2.008(3) Å] are comparable to corresponding reported distances in related complexes [70–72]; (3) Metal–oxygen bond lengths in the complexes obey the order $\text{M}-\text{OH}_2$ (1.893–2.008 Å) > $\text{M}-\text{O}_{\text{CTZ}}$ (1.842–1.909 Å) > $\text{M}-\text{O}_{\text{Ala}}$ (1.830–1.878 Å). The $\text{M}-\text{O}_{\text{CTZ}}$ bond length is longer than $\text{M}-\text{O}_{\text{Ala}}$, causing elimination of CTZ before Ala. Thus, molecular modeling calculation results are in accord with thermal analysis; (4) The bond angles in the complexes are near the perpendicular value. The $\text{O}(4)-\text{M}(7)-\text{N}(3)$, $\text{O}(8)-\text{M}(7)-\text{O}(4)$, $\text{O}(9)-\text{M}(7)-\text{O}(8)$, and $\text{O}(9)-\text{M}(7)-\text{N}(3)$ bond angles are (93.30°, 94.85°, and 93.11°), (88.53°, 91.00°, and 87.32°), (93.20°, 91.14°, and 88.89°), and (89.54°, 92.55°, and 90.49°), respectively; (5) The complexes can be arranged according to $\text{M}-\text{N}_{\text{Ala}}$ bond

Table 5. Some energies of metal complexes calculated by PM3 method.

The assignment of the theoretical parameters	The compound investigated	The theoretical data
Total energy	[Cu(CTZ)(Ala)(H ₂ O)]	= -163,527.7 (kcal M ⁻¹)
Binding energy		= -6902.6 (kcal M ⁻¹)
Electronic energy		= -1,400,557.9 (kcal M ⁻¹)
Core-core interaction		= 1,237,030.2 (kcal M ⁻¹)
Heat of formation		= -328.0 (kcal M ⁻¹)
Dipole moment		= 3.64 (Debyes)
HOMO		= -4.04
LUMO		= -0.004
Hydration energy		= -21.38 (kcal M ⁻¹)
Total energy	[Ni(CTZ)(Ala)(H ₂ O)]	= -160,266.7 (kcal M ⁻¹)
Binding energy		= -7052.0 (kcal M ⁻¹)
Electronic energy		= -1,425,600.9 (kcal M ⁻¹)
Core-core interaction		= 1,265,334.2 (kcal M ⁻¹)
Heat of formation		= -455.2 (kcal M ⁻¹)
Dipole moment		= 2.41 (Debyes)
HOMO		= -8.95
LUMO		= -0.107
Hydration energy		= -20.64 (kcal M ⁻¹)
Total energy	[Co(CTZ)(Ala)(H ₂ O)]	= -154,504.8 (kcal M ⁻¹)
Binding energy		= -7155.6 (kcal M ⁻¹)
Electronic energy		= -13,835,013.3 (kcal M ⁻¹)
Core-core interaction		= 1,190,547.8 (kcal M ⁻¹)
Heat of formation		= -519.9 (kcal M ⁻¹)
Dipole moment		= 8.2 (Debyes)
HOMO		= -4.31
LUMO		= -0.368
Hydration energy		= -19.80 (kcal M ⁻¹)

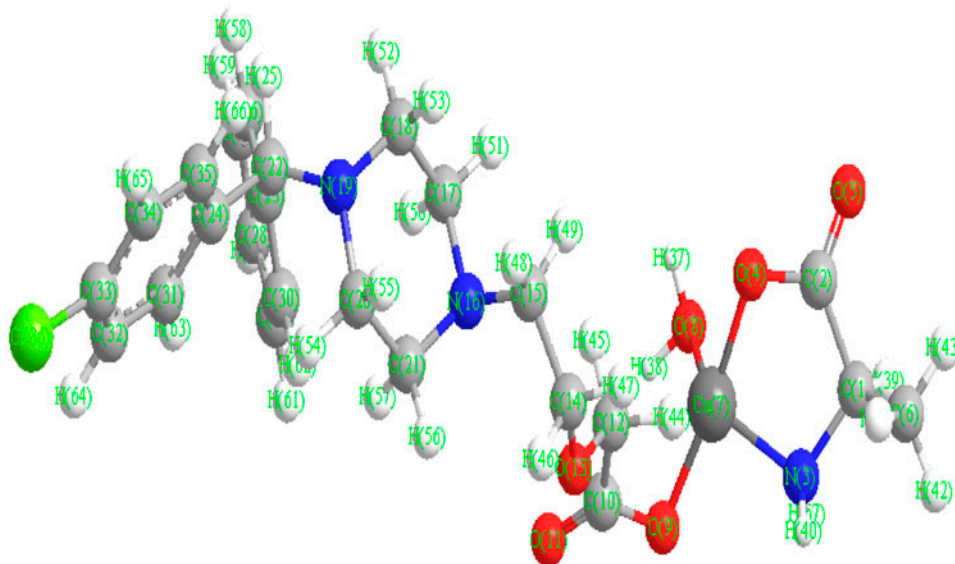
Figure 2. Optimized structure of [Cu(CTZ)(Ala)(H₂O)] with the atom numbering scheme.

Table 6. Selected bond lengths (Å) and angles (°) for the complexes.

Atoms	1	2	3
M(7)–O(8) _(H₂O)	1.961	1.893	2.008
M(7)–O(4) _(Ala)	1.873	1.830	1.878
M(7)–N(3) _(Ala)	1.914	1.844	1.905
M(7)–O(9) _(CTZ)	1.888	1.842	1.909
O(4)–M(7)–N(3)	93.30	94.85	93.11
O(8)–M(7)–O(4)	88.53	91.00	87.32
O(9)–M(7)–O(8)	93.20	91.14	88.89
O(9)–M(7)–N(3)	89.54	92.55	90.49

Ala = alanine; CTZ = cetirizine.

length, Cu–N (1.914 Å) > Co–N (1.905 Å) > Ni–N (1.844 Å), suggesting stronger Ni–N bond than the others; and (6) Finally, from elemental and thermal analyses, spectral data (infrared, electronic mass, and ESR), magnetic susceptibility measurements at room temperature, conductivity measurements, and QM calculations, a square-planar structure of the metal complexes is suggested.

3.5.2. Molecular parameters. Quantum chemical parameters of the compounds are obtained from calculations, such as the energy of the highest occupied molecular orbital, E_{HOMO} , energy of the lowest unoccupied molecular orbital, E_{LUMO} , separation energies (ΔE), absolute electronegativity (χ), ionization potential (IP), absolute hardness (η), absolute softness (σ), electron affinity (EA) [73–78], and global softness (S). The inverse of the global hardness is designated as the softness σ [79].

Equations (3)–(8) are used in calculations of molecular parameters as given below:

$$\chi = -1/2 (E_{\text{LUMO}} + E_{\text{HOMO}}) \quad (3)$$

$$\eta = 1/2 (E_{\text{LUMO}} - E_{\text{HOMO}}) \quad (4)$$

$$S = 1/2 \eta \quad (5)$$

$$\sigma = 1/\eta \quad (6)$$

Within the validity of Koopmans theorem [80], the frontier orbital energies are given by:

$$-E_{\text{HOMO}} = I \quad (7)$$

$$-E_{\text{LUMO}} = EA \quad (8)$$

From the obtained data (table 7) we deduce: (a) Absolute hardness (η) and softness (σ) measure the molecular stability and reactivity. A hard molecule has a large energy gap and a soft molecule has a small energy gap. Soft molecules are more reactive than hard ones

Table 7. The calculated quantum chemical parameters of mixed-ligand–metal complexes.

Compound	HOMO (eV)	LUMO (eV)	ΔE (eV)	IP (eV)	EA (eV)	x	η	σ	S
Cu(II)–CTZ–Ala	–4.04	–0.004	4.03	4.04	0.004	2.022	2.018	0.496	0.248
Ni(II)–CTZ–Ala	–8.95	–0.107	8.84	8.95	0.11	4.528	4.42	0.226	0.113
Co(II)–CTZ–Ala	–4.31	–0.368	3.94	4.31	0.37	2.339	1.97	0.507	0.254

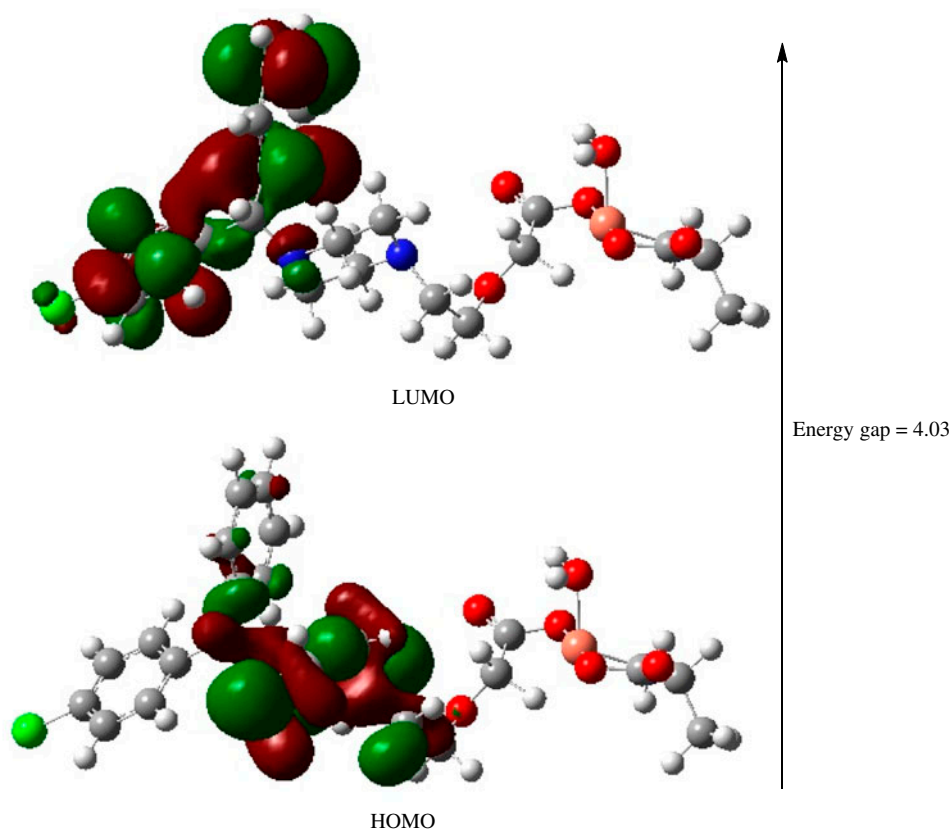


Figure 3. The atomic compositions of frontier molecular orbital and their orbital energies for $[\text{Cu}(\text{CTZ})(\text{Ala})(\text{H}_2\text{O})]$.

because they could easily offer electrons to an acceptor. Metal ions are soft acids and thus, soft base ligands are most effective for complex formation; (b) The electronic structure of the complexes was studied by analyzing the nature of the highest occupied molecular orbitals (HOMO) and lowest unoccupied molecular orbitals (LUMO). The HOMO–LUMO energy separation can be used to predict kinetic stability and reactivity pattern of the molecule. A small HOMO–LUMO gap implies a low kinetic stability and high chemical reactivity as it is energetically favorable to add electrons to LUMO or to extract electrons from a HOMO [81]. Pearson pointed out that the HOMO–LUMO energy separation represents the chemical hardness of a molecule [82]. The chemical hardness values were calculated from their HOMO and LUMO energies to predict their stability. The chemical hardness values of the metal(II) complexes, reported in table 7 [83], are in the order $[\text{Ni}(\text{CTZ})(\text{Ala})(\text{H}_2\text{O})]$ (2) > $[\text{Cu}(\text{CTZ})(\text{Ala})(\text{H}_2\text{O})]$ (1) > $[\text{Co}(\text{CTZ})(\text{Ala})(\text{H}_2\text{O})]\cdot\text{H}_2\text{O}$ (3); (c) Lower HOMO energy values show that the molecule electron donating ability is weaker and a higher HOMO energy implies that the molecule is a good electron donor, important for formation of a charge-transfer complex between molecule and biological target; (d) The value of the energy separation between the HOMO and LUMO for the Ni(II) complex is 8.84. This large HOMO–LUMO gap means high excitation energies for many of the excited

states, good stability, and a large chemical hardness for this complex [84]; (e) The electric dipole moment is a measurement of the separation of electrical charges in a system. The [Co(CTZ)(Ala)(H₂O)] complex has a large dipole (8.20) moment and [Ni(CTZ)(Ala)(H₂O)] has the smallest dipole moment (2.41); (f) The atomic compositions of frontier molecular orbital and their orbital energies for [Cu(CTZ)(Ala)(H₂O)] are shown in figure 3.

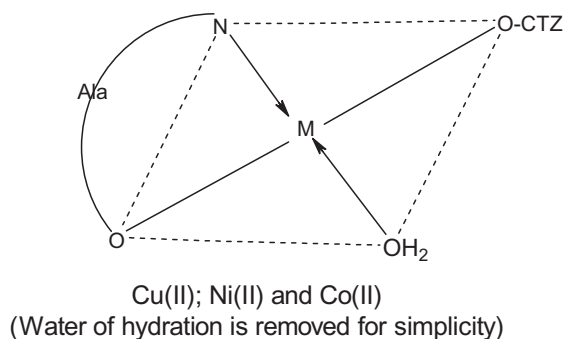
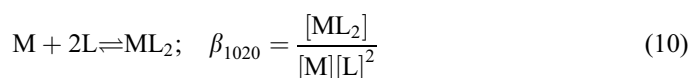
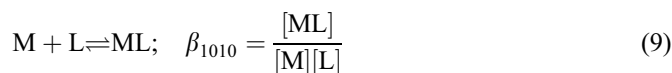
3.6. Structural interpretation

From all of the above observations and the data reported, the structures of these complexes are given in scheme 3. The structure proposed is square-planar geometry for M(II)-complexes with CTZ as mononegative, monodentate chelating ligand via carboxylate. Amino acids are coordinating via carboxylate and amino groups.

3.7. Equilibrium studies

Although data of all ligands can be found in the literature, all of them were refined in this study in order to obtain all values based on the same experimental conditions. The values found in this study (table 8) are in agreement with the ones reported [85–87].

3.7.1. Formation of binary complexes. Analysis of potentiometric titration curves in the presence of metal ions indicates that addition of metal ion to the free ligand solutions shifted the buffer region of the ligand to lower pH. The observed decrease in the binary ML curve in comparison to the free ligand solution curve indicates formation of binary complexes in solution. The formation constants of all binary complexes with CTZ and Ala were computed, taking into account all the possible species (H₂L, HL, L, M(II), ML, and ML₂). Table 8 presents the logarithms of the stability constants for all of the complex species detected by potentiometric titrations on the basis of the equilibria (9) and (10) (The charges are omitted for simplicity.).



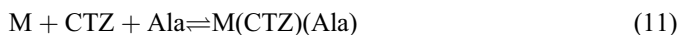
Scheme 3. Proposed structural formulae of mixed-ligand M(II) complexes.

Table 8. Protonation constants of CTZ/Ala and their binary complexes in aqueous solution at different temperatures and $I = 0.2 \text{ M dm}^{-3} \text{ NaCl}$.

Parameters	Protonation and stability constant values at different temperatures							
	288.15 K		293.15 K		298.15 K		303.15 K	
	CTZ	Ala	CTZ	Ala	CTZ	Ala	CTZ	Ala
$\log K_{\text{HL}}$	7.98 ± 0.02	9.77 ± 0.04	7.87 ± 0.03	9.68 ± 0.04	7.76 ± 0.03	9.56 ± 0.05	7.65 ± 0.07	9.45 ± 0.08
$\log K_{\text{HL}_2}$	3.26 ± 0.01	2.24 ± 0.03	3.22 ± 0.01	2.21 ± 0.03	3.19 ± 0.04	2.19 ± 0.04	3.15 ± 0.01	2.16 ± 0.09
$\log K_{\text{CuL}}$	7.13 ± 0.05	8.11 ± 0.05	7.05 ± 0.06	8.01 ± 0.01	6.96 ± 0.01	7.90 ± 0.02	6.89 ± 0.01	7.79 ± 0.03
$\log K_{\text{CuL}_2}$	4.16 ± 0.04	6.76 ± 0.07	4.11 ± 0.05	6.71 ± 0.01	4.06 ± 0.01	6.68 ± 0.04	4.02 ± 0.08	6.63 ± 0.06
$\log K_{\text{NiL}}$	6.41 ± 0.03	5.49 ± 0.01	6.34 ± 0.02	5.41 ± 0.04	6.25 ± 0.03	5.33 ± 0.05	6.16 ± 0.07	5.26 ± 0.05
$\log K_{\text{NiL}_2}$	3.46 ± 0.05	4.54 ± 0.06	3.41 ± 0.06	4.47 ± 0.03	3.36 ± 0.06	4.41 ± 0.08	3.31 ± 0.09	4.36 ± 0.04
$\log K_{\text{CoL}}$	5.33 ± 0.07	4.40 ± 0.02	5.26 ± 0.02	4.34 ± 0.08	5.19 ± 0.05	4.28 ± 0.03	5.12 ± 0.01	4.22 ± 0.05
$\log K_{\text{CoL}_2}$	3.24 ± 0.08	3.61 ± 0.03	3.20 ± 0.07	3.57 ± 0.05	3.17 ± 0.09	3.53 ± 0.08	3.14 ± 0.08	3.50 ± 0.07

Formation constants found in our study are in agreement with data in the literature [88, 89].

3.7.2. Ternary complex formation equilibria. Depending on the chelating ability of CTZ and Ala, the ternary complex formation may proceed through either a stepwise or simultaneous mechanism. The formation constants of the binary M(II)–Ala and M(II)–CTZ complexes are given in table 8. The formation constants of the binary M(II) complexes with CTZ and Ala were of the same order. Consequently, the ligation of CTZ and alanine will occur simultaneously according to the following equilibrium (11). This assumption was supported by comparing the experimental potentiometric data with the theoretically calculated (simulated) curve.



The stability constants for equilibrium (11) for mixed-ligand complexes giving the best fit of the pH-metric titration curves are listed in table 9, expressed as $\log \beta_{1110}$, calculated considering the acid dissociation constants of the ligands, and formation constants of the binary complexes as known quantities.

3.7.3. Speciation study. Estimation of equilibrium concentrations of metal(II) complexes as a function of pH provides metal ion binding in solutions. All of the species' distributions were calculated with the aid of the Species computer program [48]. The species distribution pattern for Cu–(CTZ)–Ala taken as a representative example of metal(II) mixed-ligand complexes is given in figure 4. The mixed-ligand complex Cu–(CTZ)–Ala starts to form above pH 3.5 and is up to 80–94% of the total Cu(II) ion in the pH range 7.4–8.6. Additionally, the binary Cu–CTZ and Cu–Ala systems are present in substantial amounts at lower pH with the Cu–CTZ complex forming at pH \sim 3 and reaching its maximum concentration of 50% at pH \sim 4.5, and Cu–Ala complex starts to form at pH \sim 3.2 and reaches its maximum concentration of 13% at pH \sim 4.8.

3.7.4. Correlation of the properties of metal ions with the formation constants of mixed ligand complexes. To explain why a given ligand prefers binding to one metal rather than another, it is necessary to correlate the stability constants with the characteristic properties of the metal ions, such as the ionic radius, ionization energy, electronegativity, and atomic number. Here, we discuss relationships between the properties of metal ions in the literature [90] and the stability constants of complexes. The stability constants listed in table 8 clearly show that the stability order of the binary systems in terms of metal ions is Cu(II) > Ni(II) > Co(II), and copper(II) has the highest stability of the CTZ/alanine

Table 9. Stability of mixed-ligand complexes of metal(II)–CTZ–Ala in aqueous solution at different temperatures and $I = 0.2 \text{ M dm}^{-3} \text{ NaCl}$.

Parameters	Stability constant values at different temperatures for mixed-ligand complexes			
	288.15 K	293.15 K	298.15 K	303.15 K
$\log K_{\text{Cu-CTZ-Ala}}$	14.88 ± 0.05	14.73 ± 0.06	14.55 ± 0.04	14.42 ± 0.02
$\log K_{\text{Ni-CTZ-Ala}}$	11.36 ± 0.04	11.26 ± 0.07	11.15 ± 0.03	11.05 ± 0.04
$\log K_{\text{Co-CTZ-Ala}}$	9.10 ± 0.08	8.97 ± 0.07	8.86 ± 0.05	8.76 ± 0.05

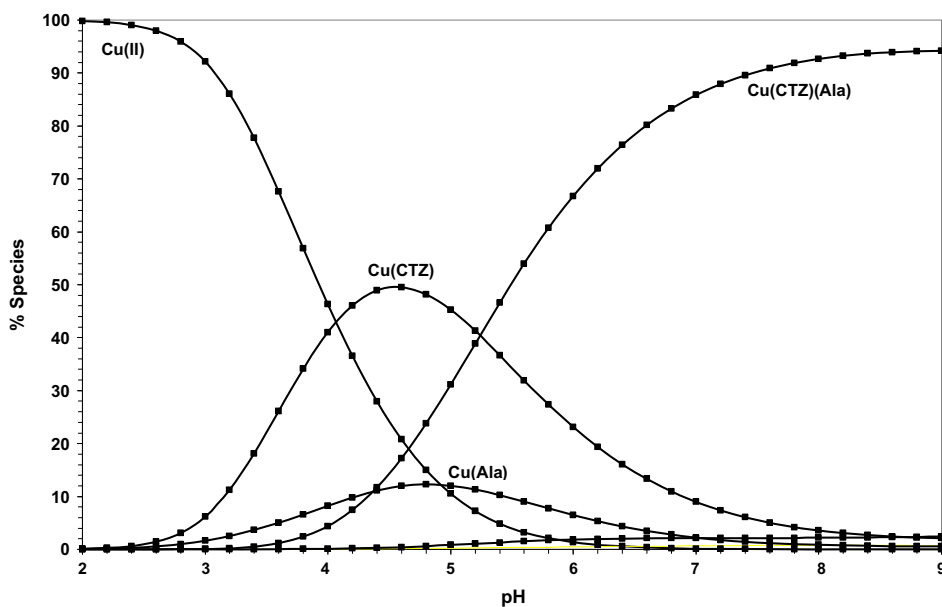


Figure 4. Concentration distribution of various species as a function of pH in the Cu-CTZ-Ala system.

complexes. There is no single factor that can explain this stability order of the complexes satisfactorily. The ratio of charge to radius is considered to be of prime importance and Cu (II) has the smallest size among the studied metal ions ($r_{\text{Cu}^{2+}} = 71$; $r_{\text{Co}^{2+}} = 72$; $r_{\text{Ni}^{2+}} = 72$) [90]. This behavior is consistent with the stability order of the binary complexes and the Irving-Williams order [91, 92]. Other possible factors are the decreasing ionic radii and the increasing ionic potentials. However, all these factors are interlinked and favor the cupric ion with which the stability is nearly always the highest in comparison to other 3d transition metals. This was reported earlier for similar systems [91]. The correlation between the $\log K_{\text{ML}}$ and the atomic number of the studied bivalent transition metal ions was found to be almost linear. Also, a good linear correlation has been obtained between $\log K_{\text{ML}}$ and the electronegativities of the metal ions. Overall formation of mixed-ligand complexes in terms of metal ions obeys this order: $\log K_{\text{Cu-CTZ-Ala}} = 14.55 > \log K_{\text{Ni-CTZ-Ala}} = 11.15 > \log K_{\text{Co-CTZ-Ala}} = 8.86$ (table 10). The sharp increase of the Cu(II) complex than other metal ion complexes is due to the Jahn-Teller effect, which will give Cu^{2+} extra stabilization due to tetragonal distortion of the octahedral symmetry [93, 94]. With respect to increasing electronegativity (E.N.) of the metals, the electronegativity difference between metal atom ($E.N_{\text{Cu(II)}} = 2.00$; $E.N_{\text{Ni(II)}} = 1.91$ and $E.N_{\text{Co(II)}} = 1.88$) and donor ($E.N_{\text{Oxygen}} = 3.5$ and $E.N_{\text{Nitrogen}} = 3.0$) of the ligand will decrease; hence, the metal-ligand bond would have more covalent character which may lead to stability of metal chelates.

3.7.5. Comparison of the stability constant of the ternary complexes with those of the binary complexes. The stability of mixed-ligand complexes with respect to the corresponding binary analogs can be articulated quantitatively in terms of $\Delta \log K$, $\log X$, and $\Delta \log \beta$ parameters as follows:

Table 10. Values of $\log \beta$; $\Delta \log K$; $\Delta \log \beta$ and $\log X$ for formation of the ternary complexes at 0.2 M NaCl at 25 °C.

Complex	$\log \beta_{1110}$ (experimentally)	$\log \beta_{1010}$	$\log \beta_{1020}$	$\Delta \log K^a$	$\log X^b$	$\log \beta_{\text{stat}}^c$	$\Delta \log \beta^d$
Cu-CTZ-Ala	14.55	7.90	14.58	-0.31	3.5	13.10	1.45
Ni-CTZ-Ala	11.15	5.33	9.74	-0.43	2.95	9.98	1.17
Co-CTZ-Ala	8.86	4.28	7.81	-0.61	1.55	8.39	0.47

^a $\Delta \log K = \log \beta_{1110} - \log \beta_{1100} - \log \beta_{1010}$; ^b $\log X = (2 \log \beta_{1110} - \log \beta_{1020} - \log \beta_{1200})$; ^c $\log \beta_{\text{stat}} = \log 2 + 1/2 \log \beta_{1020} + 1/2 \log \beta_{1200}$; ^d $\Delta \log \beta = \log \beta_{1110} - \log \beta_{\text{stat}}$.

3.7.5.1. *$\Delta \log K$ parameter.* $\Delta \log K$ represents the difference between the stabilities of the binary and mixed-ligand complexes. One expects to obtain negative values for $\Delta \log_{10} K$ (table 10), since more coordination positions are available for the bonding of ligand (L) in the binary than in the ternary complexes. According to Sigel [95], the relative stability of a ternary complex $M(\text{CTZ})L$ (1110) compared to its binary complexes $M(\text{CTZ})$ (1100) and $M(L)$ (1010) can be expressed quantitatively by the following equations:



$$\Delta \log K_{M(\text{CTZ})\text{Ala}} = \log \beta_{M(\text{CTZ})\text{Ala}} - (\log \beta_{M(\text{CTZ})} + \log \beta_{M(\text{Ala})}) \quad (13)$$

$\Delta \log K$ has been widely accepted and used for many years [93] and the advantages in using $\Delta \log K$ in comparing stabilities of ternary and binary complexes have been reviewed. The parameter $\Delta \log K$ expresses the effect of the bound primary ligand toward an incoming secondary ligand. Since the alanine coordinates more easily with the free metal ion M^{2+} than with the complexed metal ion $[M(\text{CTZ})]^+$ in which the Lewis-acidity of metal(II) ion is depressed, the value of $\Delta \log K$ should be negative and generally have a value between -0.5 and -2.0 [95, 96], depending on the geometry of the complex. Values of $\Delta \log K$ for the ternary complexes studied in this article are listed in table 10. The tendency to form ternary complexes was compared with these values, so that if $\Delta \log K$ is less negative, this should be taken to indicate that the ternary complex is favored. The $\Delta \log K$ values of mixed-ligand complexes with Ala are less negative (-0.31 to -0.61) than the theoretical value. This may be considered as evidence for enhanced stabilities of the formed ternary complexes due to the interligand interactions that exists between CTZ and Ala with metal ions.

3.7.5.2. *Disproportionation constant ($\log X$).* The quantitative stabilization of ternary complexes can be expressed in terms of their disproportionation constant (X). The values of $\log X$ (table 10) can be calculated by equations (14) and (15)] for $M(\text{CTZ})\text{Ala}$ complexes.

$$M(\text{CTZ})_2 + M(\text{Ala})_2 \rightleftharpoons 2M(\text{CTZ})(\text{L}); X_{M(\text{CTZ})(\text{Ala})} = \frac{[M(\text{CTZ})(\text{L})]^2}{[M(\text{CTZ})_2][M(\text{L})_2]} \quad (14)$$

$$\log X_{M(\text{CTZ})(\text{Ala})} = 2 \log \beta_{M(\text{CTZ})(\text{Ala})} - (\log \beta_{M(\text{CTZ})_2} - \log \beta_{M(\text{Ala})_2}) \quad (15)$$

The value for $\log X$ expected from statistical reasons is +0.6 [97] for all geometries. The values of $\log X$ in table 10 are $\gg +0.6$, indicating marked stabilities of the ternary

complexes from interligand electronic and steric interactions in these complexes [98], indicating preference for formation of mixed-ligand M–CTZ–Ala complexes over binary complexes.

3.7.5.3. *Stabilization constant ($\Delta \log \beta$)*. The stabilization constant ($\Delta \log \beta$) results from the difference of the stability constant measured for the mixed complex and that calculated from statistical grounds. The stability of the ternary complexes investigated can also be calculated using a statistical method [99], according to the following equation:

$$\log \beta_{\text{stat}} = \log 2 + 1/2 \log \beta_{\text{M(CTZ)}_2} + 1/2 \log \beta_{\text{M(Ala)}_2} \quad (16)$$

The values of $\log \beta_{\text{stat}}$ for the mixed-ligand complexes detected in this study are shown in table 10. The large differences of $\Delta \log \beta$ values ($\log \beta_{1110} - \log \beta_{\text{stat}}$) indicate that the M (CTZ)L system is more stable than both M(CTZ)₂ and M(L)₂.

3.8. Effect of temperature and thermodynamics

The values obtained for the thermodynamic parameters ΔH° , ΔS° , and ΔG° , associated with the protonation of CTZ/Ala, their complex formation with M(II) species, and ternary complex formation were calculated from the temperature dependence of the data in tables 8 and 9. The observed protonation constant values of CTZ and Ala decrease with rise in temperature, which indicates increasing acidic nature. The same trend was observed for both the binary and mixed-ligand–Cu(II) systems. The change in free energy (ΔG), enthalpy (ΔH), and entropy (ΔS) of the above systems were evaluated using the following equations:

$$\Delta G = -2.3030 RT \log K = \Delta H - T\Delta S \quad (17)$$

$$\log K = \frac{-\Delta H}{2.303RT} + \frac{-\Delta S}{2.303R} \quad (18)$$

$$\Delta S = \frac{\Delta H - \Delta G}{T} \quad (19)$$

Van't Hoff plot was obtained by linear least squares fit of $\ln K$ versus $1/T$. The change in enthalpy (ΔH) of the systems was calculated from the slope ($-\Delta H^\circ/R$) and the change in entropy (ΔS) was calculated from the intercept ($\Delta S^\circ/R$) of the Van't Hoff plot. The main conclusions from the data can be summarized as: (I) The protonation reaction ($L + H \rightleftharpoons HL$) of the CTZ/Ala is exothermic with a net negative ΔG° . Three factors affect the protonation reactions: (i) the neutralization reaction, which is an exothermic reaction process, (ii) desolvation of ions, which is an endothermic process, and (iii) the change of the configuration and the arrangements of the hydrogen bonds around the free and protonated ligands. (II) In most cases, the color of the solution after complex formation was different from the color of the ligand at the same pH. (III) The stability constants of the M(II)-complexes formed at different temperatures were calculated and the following conclusions can be reached. These values decrease with increasing temperature, confirming that the complexation process is more favorable at lower temperature. Divalent metal ions exist in solution as octahedral hydrated species [100] and the obtained values of ΔH and ΔS can be considered as sum of two contributions: (a) release of H₂O molecules and (b) metal–ligand

Table 11. Thermodynamics of protonation constants of CTZ/Ala compounds and their binary complex formation in aqueous solution at different temperatures and $I = 0.2 \text{ M dm}^{-3} \text{ NaCl}$.

Species	System	Thermodynamic parameters									
		$\Delta G \text{ (kJ M}^{-1}\text{)}$					$\Delta H \text{ (kJ M}^{-1}\text{)}$	$\Delta S \text{ (J K}^{-1} \text{ M}^{-1}\text{)}$			
		288.15	293.15	298.15	303.15	288.15		293.15	298.15	303.15	
H ₂ L	HCTZ	-44.03	-44.17	-44.3	-44.40	-36.79	25.12	25.19	25.20	25.12	
	H ₂ CTZ	-17.99	-18.07	-18.21	-18.28	-12.04	20.63	20.58	20.70	20.60	
	HAla	-53.90	-54.33	-54.58	-54.85	-36.10	61.79	62.21	61.97	61.80	
	H ₂ Ala	-12.36	-12.40	-12.50	-12.54	-8.70	12.71	12.65	12.77	12.67	
M-CTZ	Cu-CTZ	-39.34	-39.57	-39.73	-39.99	-27.10	42.46	42.54	42.36	42.52	
	Cu(CTZ) ₂	-22.95	-23.07	-23.18	-23.33	-15.73	25.06	25.03	24.98	25.08	
	Ni-CTZ	-35.37	-35.59	-35.69	-35.76	-28.07	25.31	25.64	25.52	25.35	
	Ni(CTZ) ₂	-19.09	-19.14	-19.18	-19.21	-16.72	8.21	8.25	8.25	8.21	
M- α -Ala	Co-CTZ	-29.41	-29.52	-29.63	-29.73	-23.41	20.81	20.85	20.85	20.81	
	Co(CTZ) ₂	-17.88	-17.96	-18.10	-18.23	-11.05	23.69	23.58	23.64	23.68	
	Cu(Ala)	-44.74	-44.96	-45.10	-45.22	-35.78	31.13	31.33	31.27	31.14	
	Cu(Ala) ₂	-37.3	-37.66	-38.13	-38.48	-14.05	80.68	80.56	80.79	80.61	
	Ni(Ala)	-30.29	-30.37	-30.43	-30.53	-25.76	15.71	15.7	15.64	15.73	
	Ni(Ala) ₂	-25.05	-25.09	-25.18	-25.31	-20.09	17.21	17.06	17.06	17.21	
M-CTZ- α -Ala	Co(Ala)	-24.28	-24.36	-24.43	-24.49	-20.07	14.61	14.64	14.64	14.61	
	Co(Ala) ₂	-19.92	-20.04	-20.15	-20.32	-12.39	26.14	26.10	26.05	26.16	
	Cu-CTZ- α -Ala	-82.10	-82.68	-83.06	-83.7	-52.20	103.76	103.98	103.52	103.92	
	Ni-CTZ- α -Ala	-62.68	-63.20	-63.65	-64.14	-34.78	96.80	96.94	96.83	96.84	
	Co-CTZ- α -Ala	-50.21	-50.35	-50.58	-50.85	-37.83	42.96	42.71	42.77	42.95	

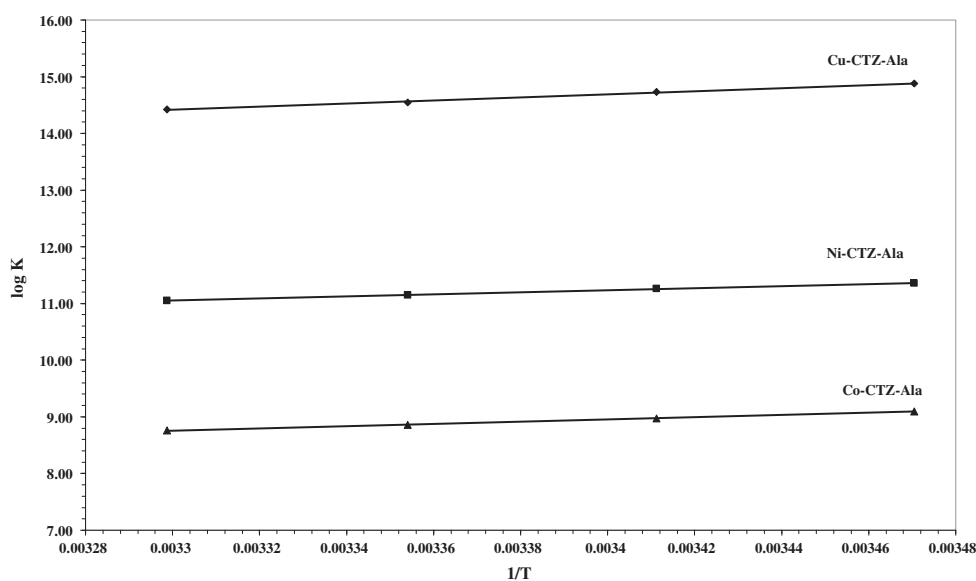


Figure 5. The stability constants of the mixed-ligand M-(CTZ)-Ala complexes formed at different temperatures.

bond formation. From these results, the following conclusions can be made: (a) The difference between the stability constants of 1 : 1 and 1 : 2 complexes is usually positive (0.72–0.79), (0.90–0.95), (1.22–1.49), (1.98–2.09), (2.85–2.95), and (2.87–2.97) for Co–Ala, Ni–Ala, Cu–Ala, Co–CTZ, Ni–CTZ, and Cu–CTZ, respectively. This may be attributed to the coordination sites of the metal ions more freely available for binding of the first molecule than the second one. (b) All the binary systems show positive entropy (ΔS) values, which indicate the complexation is entropically favorable under the experimental conditions. The positive value of entropy is attributed to increased disorder as a result of desolvation and release of bound solvent molecules on chelation is greater than the decrease resulting from the chelation process itself. It occurs because the solvent molecules are arranged in an orderly fashion around the ligand, and the metal ion has acquired a more random configuration on chelation [101]. (c) The calculated thermodynamic parameters are collected in table 11 and the representative van't Hoff plot for mixed-ligand complexes ($\log K$ versus $1/T$) is displayed in figure 5. (d) In M–CTZ–Ala mixed-ligand systems, the stability constant values decrease with increase in temperature as shown in figure 5. (e) For the same ligand at constant temperature, the stability of the chelates increases in the order $\text{Cu}^{2+} > \text{Ni}^{2+} > \text{Co}^{2+}$ [102]. This order largely reflects the changes in the heat of complex formation across the series from a combination of the influence of both the polarizing ability of the metal ion [103] and the crystal field stabilization energies [100]. (f) All values of ΔG for complexation are negative (table 11), indicating that the chelation process proceeds spontaneously. (g) The negative values of ΔH° show that the chelation process is exothermic, indicating that the complexation reactions are favored at low temperature. (h) Release of solvent from the systems leads to a stable metal–ligand chelation and hence, there is a large positive ΔS . (i) The complexation of CTZ with M(II) ion in the presence of Ala is entropically favorable (table 11). (j) It is generally noted that $-\Delta G_1 > -\Delta G_2^\circ$ and $-\Delta H_1 > -\Delta H_2^\circ$ (table 11), attributed to steric hindrance produced by the second molecule.

3.9. Biological activity

To assess the biological potential of the synthesized compounds, CTZ and its metal complexes were tested against different species of bacteria and fungi. All of the tested compounds showed activity against different types of gram-positive (*Bacillus subtilis* RCMB 010067, *Staphylococcus aureus* RCMB 010028) and gram-negative bacteria (*Pseudomonas aeruginosa* RCMB 010043, *Escherichia coli* RCMB 010052) and (*Aspergillus flavus* RCMB 02568, *Penicillium italicum* RCMB 03924, *Candida albicans* RCMB 05031, *Geotricum candidum* RCMB 05097) fungus. The data are listed in tables 12 and 13. On comparing the biological activity of CTZ and its metal complexes, the following results are obtained: (1) CTZ and its metal complexes have no biological activity against *Pseudomonas aeruginosa*. (2) Antibacterial activity of metal complexes follow the order Ni(II) > Cu(II) > Co(II) (figure 6). (3) The activity index for Ni(II) complex is 77.13, 69.14, and 83.94% toward *Escherichia coli* RCMB010052; *Bacillus subtilis* RCMB010067, and *Staphylococcus aureus* RCMB010028, respectively. (4) The tested complexes were more active against gram-positive than gram-negative bacteria. Gram-positive bacteria possess a thick cell wall containing many layers of peptidoglycan and teichoic acids, but in contrast, gram-negative bacteria have a relatively thin cell wall consisting of a few layers of peptidoglycan surrounded by a second lipid membrane containing lipopolysaccharides and lipoproteins. These differences in cell wall structure can produce differences in antibacterial susceptibility

Table 12. Antibacterial activity and activity index of M(II)-CTZ-Ala complexes.

Compounds	Bacterial species							
	G^-				G^+			
	<i>Pseudomonas aeruginosa</i> RCMB010043		<i>Escherichia coli</i> RCMB010052		<i>Bacillus subtilis</i> RCMB010067		<i>Staphylococcus aureus</i> RCMB010028	
	Zone (mm) ^a	Activity index	Zone (mm)	Activity index	Zone (mm)	Activity index	Zone (mm)	Activity index
CTZ	NA	–	8.6 ± 0.6	38.57	12.6 ± 0.3	37.84	10.5 ± 0.2	38.36
Cu-CTZ-Ala	NA	–	11.8 ± 0.5	52.91	13.9 ± 0.3	42.90	15.6 ± 0.4	56.93
Ni-CTZ-Ala	NA	–	17.2 ± 0.3	77.13	22.4 ± 0.6	69.14	23.0 ± 0.4	83.94
Co-CTZ-Ala	NA	–	10.4 ± 0.6	46.64	14.9 ± 0.6	45.99	12.6 ± 0.4	43.43
Standard ^b	17.3 ± 0.15	–	22.3 ± 0.2	–	32.4 ± 0.1	–	27.4 ± 0.2	–

^aZone: Diameter of inhibition zone in mm; ^bStandard: Gentamicin and Ampicillin for G^- and G^+ bacterial species, respectively.

Table 13. Antifungal activity and activity index of M(II)-CTZ-Ala complexes.

Compounds	Fungal species							
	<i>Aspergillus flavus</i> RCMB010043		<i>Penicillium italicum</i> RCMB010052		<i>Candida albicans</i> RCMB010067		<i>Geotricum candidum</i> RCMB010028	
	Zone (mm) ^a	Activity index	Zone (mm)	Activity index	Zone (mm)	Activity index	Zone (mm)	Activity index
	CTZ	12.4 ± 0.4	52.41	14.6 ± 0.6	63.48	NA	–	14.4 ± 0.3
Cu-CTZ-Ala	15.8 ± 0.3	66.67	16.3 ± 0.2	70.87	NA	–	17.8 ± 0.4	62.02
Ni-CTZ-Ala	19.7 ± 0.3	83.12	18.1 ± 0.2	78.70	NA	–	21.3 ± 0.4	74.22
Co-CTZ-Ala	14.6 ± 0.4	63.16	13.2 ± 0.7	57.39	NA	–	15.3 ± 0.5	53.31
Standard ^b	23.7 ± 0.1	–	21.9 ± 0.1	–	19.8 ± 0.20	–	28.7 ± 0.2	–

^aZone: Diameter of inhibition zone in mm; ^bStandard: Amphotericin for fungal species.

[33, 53, 104]. (5) The synthesized complexes were more toxic compared with CTZ against the same micro-organism under the same experimental conditions. The increase in biological activity of the metal chelates may be due to the effect of the metal ion on the normal cell process. A possible mode of toxicity increase may be considered in the light of Tweedy's chelation theory [105]. Also, it is proposed that the action of the toxicant is denaturation of one or more proteins of the cell, impairing normal cellular process [106]. These results agree with similar studies for mixed-ligand complexes [33, 107–109]. (6) Antifungal activity of CTZ and its metal complexes is not observed toward *Candida albicans* RCMB010067. (7) Ni(II) complex showed higher antifungal activity among the synthesized complexes against all selected types of fungi (figure 7). (8) The activity index for Ni(II) complex is 83.12, 78.70, and 74.22% toward *Aspergillus flavus* RCMB010043, *Penicillium italicum* RCMB010052, and *Geotricum candidum* RCMB010028, respectively. (9) Ni(II) complex is the most promising broad spectrum antimicrobial complex versus *Aspergillus flavus* RCMB010043 and *Staphylococcus aureus* RCMB010028 with activity index of 83.1 and 83.94%, respectively, while Co(II) complex has the lowest antimicrobial activity antimicrobial complex among the synthesized complexes versus *Geotricum candidum* RCMB010028 and *Staphylococcus aureus* RCMB010028 with activity index of 53.31% and 43.43%, respectively. (10) Cu(II) complex has moderate biological activity versus *Staphylococcus aureus* RCMB010028 and *Penicillium italicum* RCMB010052 with activity index of 56.93% and 70.87%, respectively.

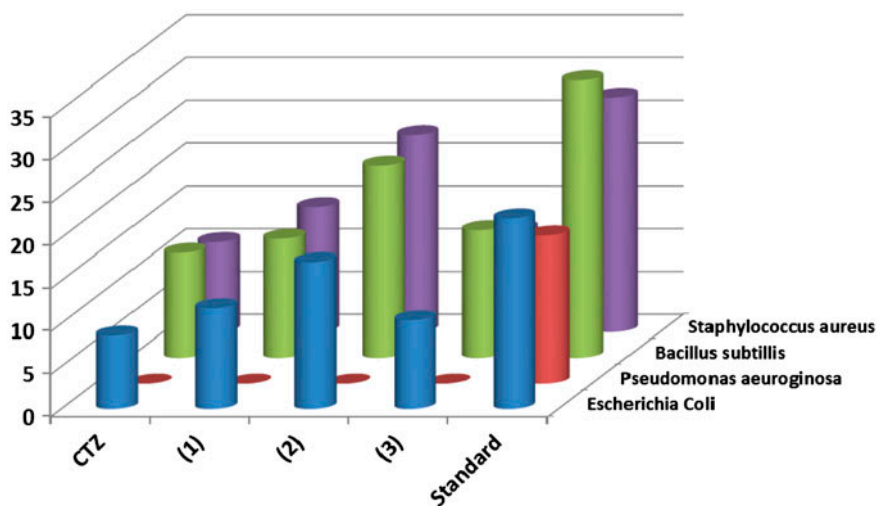


Figure 6. Antibacterial activity of M-CTZ-Ala complexes.

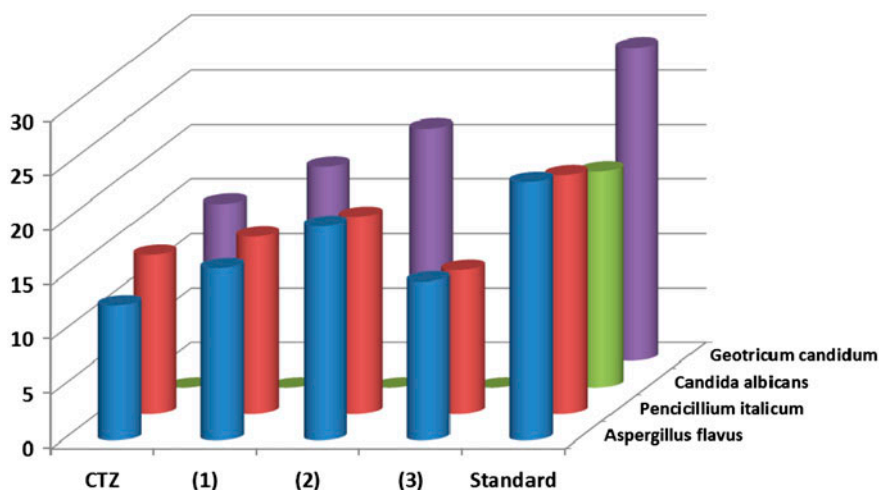


Figure 7. Antifungal activity of M-CTZ-Ala complexes.

3.9.1. Antibacterial activity and physicochemical properties of the synthesized compounds. SAR studies suggest an inverse correlation between the dipole moment and the activity of complexes against bacterial species. As dipole moment decreases the polarity decreases and in turn the lipophilic nature of the compound increases, which favors permeation through the lipid layer of the micro-organism [110]. From the data given in table 7, $[\text{Ni}(\text{CTZ})(\text{Ala})(\text{H}_2\text{O})]$ has a lower dipole moment ($\mu = 2.41$), thus it has a more lipophilic nature and a higher biological activity than the other complexes. The lipophilicity of the M (II) complexes obeys this order: $[\text{Ni}(\text{CTZ})(\text{Ala})(\text{H}_2\text{O})] > [\text{Cu}(\text{CTZ})(\text{Ala})(\text{H}_2\text{O})] > [\text{Co}(\text{CTZ})(\text{Ala})(\text{H}_2\text{O})] \cdot \text{H}_2\text{O}$, indicating lower values of dipole moment contribute to higher antibacterial activity.

[Ni(CTZ)(Ala)(H₂O)] (**2**) (HOMO = -8.95), which presented the lowest value of HOMO, showed the highest activity against the selected types of bacterial and fungal species [111].

4. Conclusion

The present article reports synthesis and characterization of M-CTZ-Ala complexes. The synthetic procedure in this work resulted in the formation of complexes in the molar ratio (1 : 1 : 1) (M : CTZ : Ala). In these complexes, the cetirizine is a monodentate negatively charged ligand coordinated to metal ion through the carboxylate oxygen. The alanine is a bidentate negatively charged ligand coordinated to metal ion through the carboxylate oxygen and amino groups. The complexes are nonelectrolytes with square-planar geometry around M(II). Stability of the mixed-ligand complexes is mainly affected by the characteristics of Ala. The less negative $\Delta \log K$ and more positive $\log X$ values indicate the stabilities of these mixed-ligand complexes. The biological activities of the isolated metal chelates were screened against different types of bacteria and fungi. CTZ and the complexes inhibited the growth of tested bacteria to varying degrees, more pronounced when coordinated to the metal ions. The antibacterial activity of all the complexes follow the order Ni(II) > Cu(II) > Co(II), suggesting metal chelation significantly affects the antimicrobial behavior. The metal complexes exhibit antimicrobial properties with enhanced inhibitory activity compared to the parent ligand under identical experimental conditions. The antibacterial activity has been explained on the basis of chelation theory. The complexes were more active against gram-positive than gram-negative bacteria. It may be concluded that antibacterial activity of the compounds is related to cell wall structure of the bacteria. The Ni(II) complex is the most promising potent broad spectrum antimicrobial compound among the complexes.

Acknowledgement

The authors express their sincere thanks to the Northern Border University for financial support of the project number (435-077-8).

References

- [1] R.M. Roat-Malone. *Bioinorganic Chemistry*, Wiley, Hoboken, NJ (2002).
- [2] R.R. Crichton. *Biological Inorganic Chemistry An Introduction*, Elsevier, Amsterdam (2008).
- [3] O. Prakash, R. Kumar, R. Kumar, P. Tyagi, R.C. Kuhad. *Eur. J. Med. Chem.*, **42**, 868 (2007).
- [4] N. Zhang, S. Ayril-Kaloustian, T. Nguyen, R. Hernandez, C. Beyer. *Bioorg. Med. Chem. Lett.*, **17**, 3003 (2007).
- [5] M.C. Lanier, M. Feher, N.J. Ashweek, C.J. Loweth, J.K. Rueter, D.H. Slee, J.P. Williams, Y.F. Zhu, S.K. Sullivan, M.S. Brown. *Bioorg. Med. Chem.*, **15**, 5590 (2007).
- [6] J.M.C. Howell, J.M. Gawthorne. *Copper in Animals and Man*, Vols. 1 and 2, 1st Edn, CRC Press, Boca Raton, FL (1987).
- [7] A.A. El-Sherif, M.R. Shehata, M.M. Shoukry, M.H. Barakat. *Spectrochim. Acta, Part A*, **96**, 889 (2012).
- [8] A.A. El-Sherif, M.S. Aljahdali. *J. Coord. Chem.*, **66**, 3423 (2013).
- [9] A.A. El-Sherif. *J. Coord. Chem.*, **64**, 2035 (2011).
- [10] M.S. Aljahdali, A.A. El-Sherif, R.H. Hilal, A.T. Abdel-Karim. *Eur. J. Chem.*, **4**, 370 (2013).
- [11] N.M. Urquiza, M.S. Islas, M.L. Dittler, M.A. Moyano, S.G. Manca, L. Lezama, T. Rojo, J.J.M. Medina, M. Diez, L.L. Tevez, P.A.M. Williams, E.G. Ferrer. *Inorg. Chim. Acta*, **405**, 243 (2013).

- [12] K. Alomar, A. Landreau, M. Kempf, M.A. Khan, M. Allain, G. Bouet. *J. Inorg. Biochem.*, **104**, 397 (2010).
- [13] J. Joseph, K. Nagashri, G.B. Janaki. *Eur. J. Med. Chem.*, **49**, 151 (2012).
- [14] M.A. Agotegaray, M. Dennehy, M.A. Boeris, M. Grela, R.A. Burrow, O.V. Quinzani. *Polyhedron*, **34**, 74 (2012).
- [15] Agency for Toxic Substances and Diseases Registry. *Toxicological Profile for Cobalt*, US Department of Health and Human Services, Atlanta (2004).
- [16] R.A. Poellot, T.R. Shuler, E.O. Uthus, F.H. Nielsen. *Proc. Natl Acad. Sci. USA*, **44**, 80 (1990).
- [17] F.H. Nielsen. *J. Nutr.*, **110**, 965 (1980).
- [18] A.F. Kolodziej. In *Progress in Inorganic Chemistry*, K.D. Karlin (Ed.), Vol. 41, p. 493, Wiley, New York, (1994).
- [19] K. Asemave, S.G. Yiase, S.O. Adejo, B.A. Anhwange. *Int. J. Inorg. Bioinorg. Chem.*, **2**, 11 (2011).
- [20] R.H. Garret, C.M. Grisham. *Biochemistry*, p. 216, Sanders, New York (1995).
- [21] J.H. Ottawa, D.K. Apps. *Biochemistry*, ELBS, London (1984).
- [22] T.R. Rap, M. Sahay, R.C. Aggarwal. *Ind. J. Chem.*, **23**, 214 (1984).
- [23] A. Marcu, A. Stanilaa, O. Cozar, L. David. *J. Optoelectron. Adv. Mater.*, **10**, 830 (2008).
- [24] C. Auclair, E. Voisin, H. Banoun, C. Paoletti, J. Bernadou, B. Meunier. *J. Med. Chem.*, **27**, 1161 (1984).
- [25] Y. Baran, S. Baran, N.K. Tunalı. *Turk. J. Chem.*, **21**, 105 (1997).
- [26] L.R. Dinelli, T.M. Bezerra, J.J. Sene. *Curr. Res. Chem.*, **2**, 18 (2010).
- [27] S.S. Dara. *A Textbook of Environmental Chemistry and Pollution Control*, pp. 67–69, S. Chand and Company Ltd., India (2005).
- [28] K. Pisarewicz, D. Mora, F.C. Pflueger, G.B. Fields, F. Mari. *J. Am. Chem. Soc.*, **127**, 6207 (2005).
- [29] D.S. Sigman, A. Mazumder, D.M. Perrin. *Chem. Rev.*, **93**, 2295 (1993).
- [30] L. Pearson, C.B. Chen, R.P. Gaynor, D.S. Sigman. *Nucleic Acids Res.*, **22**, 2255 (1994).
- [31] Á. García-Raso, J.J. Fiol, B. Adrover, P. Tauler, A. Pons, I. Mata, E. Espinosa, E.R. Molins. *Polyhedron*, **22**, 3255 (2003).
- [32] N.A. Al-Awadi, N.M. Shuaib, A. Abbas, A.A. El-Sherif, A. El-Dissouky, E. Al-Saleh. *Bioinorg. Chem. Appl.*, **2008**, 10 (2008). doi:10.1155/2008/479897.
- [33] A. El-Dissouky, N. Shuaib, N.A. Al-Awadi, A. Abbas, A.A. El-Sherif. *J. Coord. Chem.*, **61**, 579 (2008).
- [34] M.S. Aljahdali, A.T. Abdelkarim, A.A. El-Sherif. *J. Solution Chem.*, **42**, 2240 (2013).
- [35] M. Aljahdali, A.A. El-Sherif, M.M. Shoukry, S.E. Mohamed. *J. Solution Chem.*, **42**, 1028 (2013).
- [36] A.A. El-Sherif, M.M. Shoukry, M.M.A. Abd-Elgawad. *J. Solution Chem.*, **42**, 412 (2013).
- [37] M. Aljahdali, A.A. El-Sherif. *J. Solution Chem.*, **41**, 1759 (2012).
- [38] A.A. El-Sherif. *J. Solution Chem.*, **41**, 249 (2012).
- [39] B. Jeragh, D. Al-Wahaib, A.A. El-Sherif, A. El-Dissouky. *J. Chem. Eng. Data*, **52**, 1609 (2007).
- [40] *HyperChem version 7.5*, Hypercube, Inc., Gainesville, FL, (2003).
- [41] A.W. Bauer, W.M. Kirby, C. Sherris, M. Turck. *J. Am. Clin. Path.*, **45**, 493 (1966).
- [42] M.A. Pfäller, L. Burmeister, M.A. Bartlett, M.G. Rinaldi. *J. Clin. Microbiol.*, **26**, 1437 (1988).
- [43] National Committee for Clinical Laboratory Standards. *Methods for Dilution Antimicrobial Susceptibility Tests for Bacteria that Grow Aerobically*, Approved Standard M7-A3, Villanova, PA (1993).
- [44] L.D. Liebowitz, H.R. Ashbee, E.G.V. Evans, Y. Chong, N. Mallatova, M. Zaidi, D. Gibbs. *Diagn. Microbiol. Infect. Dis.*, **40**, 27 (2001).
- [45] M.J. Matar, L. Ostrosky-Zeichner, V.L. Paetznick, J.R. Rodriguez, E. Chen, J.H. Rex. *Antimicrob. Agents Chemother.*, **47**, 1647 (2003).
- [46] A.A. El-Sherif. *J. Coord. Chem.*, **64**, 1240 (2011).
- [47] P. Gans, A. Sabatini, A. Vacca. *Inorg. Chim. Acta*, **18**, 237 (1976).
- [48] L.Pettit. University of Leeds, Personal Communication.
- [49] F. Dimiza, A.N. Papadopoulos, V. Tangoulis, V. Psycharis, C.P. Raptopoulou, D.P. Kessissoglou, G. Psomas. *J. Inorg. Biochem.*, **107**, 54 (2012).
- [50] R.C. Mehrotra, R. Bohra. *Metal Carboxylates*, Academic Press, New York (1983).
- [51] N.B. Colthup, L.H. Daly, S.E. Wiberley. *Introduction to Infrared and Raman Spectroscopy*, 3rd Edn, Academic Press, Boston, MA (1990).
- [52] G.B. Deacon, R.J. Philips. *J. Coord. Rev.*, **33**, 227 (1980).
- [53] A.A. El-Sherif, M.M. Shoukry, L.O. Abobakr. *Spectrochim. Acta, Part A*, **112**, 290 (2013).
- [54] K. Nakamoto. *Infrared and Raman Spectra of Inorganic and Coordination Compounds*, 4th Edn, Wiley, New York (1986).
- [55] A.A. El-Sherif. *J. Solution Chem.*, **39**, 1562 (2010).
- [56] J. Sanmartín, M.R. Bermejo, A.M. Garia-Deibe, M. Maneiro, C. Lage, J. Costa-Filho. *Polyhedron*, **19**, 185 (2000).
- [57] A.P. Mishra. *J. Indian Chem. Soc.*, **76**, 35 (1999).
- [58] W.J. Geary. *J. Coord. Chem. Rev.*, **7**, 81 (1971).
- [59] L.K. Thompson, F.L. Lee, E.J. Gabe. *Inorg. Chem.*, **27**, 39 (1988).
- [60] A.B.P. Lever. *Inorganic Electronic Spectroscopy*, Elsevier, Amsterdam (1984).
- [61] A.A. El-Sherif, T.M.A. Eldebss. *Spectrochim. Acta, Part A*, **79**, 1803 (2011).

- [62] G. Ertem, D.X. West. *Transition Met. Chem.*, **9**, 412 (1984).
- [63] M. Nonoyama, K. Yamasaki. *Inorg. Chim. Acta*, **5**, 124 (1971).
- [64] A.T. Karim, A.A. El-Sherif. *Eur. J. Chem.*, **5**, 328 (2014).
- [65] D.N. Sathyanarayana. *Electronic Absorption Spectroscopy and Related Techniques*, Orient Longman Limited, Universities Press (India) Limited (2001).
- [66] Y. Nishida, S. Kida. *Coord. Chem. Rev.*, **27**, 275 (1979).
- [67] K. Singh, M.S. Barwa, P. Tyagi. *Eur. J. Med. Chem.*, **42**, 394 (2007).
- [68] R.L. Dutta, A. Syamal. *Elements of Magnetochemistry*, 2nd Edn, Affiliated East-West Press, New Delhi (1993).
- [69] A.A. El-Sherif. *J. Solution Chem.*, **39**, 1562 (2010).
- [70] Y. Nishida, S. Kida. *J. Chem. Soc., Dalton Trans.*, 2633 (1986).
- [71] Y. Song, C. Massera, O. Roubeau, P. Gamez, A.M.M. Lanfredi, J. Reedijk. *J. Inorg. Chem.*, **43**, 6842 (2004).
- [72] D.X. West, J.K. Swearingen, J. Valdés-Martínez, S. Hernández-Ortega, A.K. El-Sawaf, F. van Meurs, A. Castiñeiras, I. Garcia, E. Bermejo. *Polyhedron*, **18**, 2919 (1999).
- [73] R.G. Pearson. *J. Org. Chem.*, **54**, 1423 (1989).
- [74] R.G. Parr, R.G. Pearson. *J. Am. Chem. Soc.*, **105**, 7512 (1983).
- [75] P. Geerlings, F. De Proft, W. Langenaeker. *Chem. Rev.*, **103**, 1793 (2003).
- [76] R.G. Parr. *J. Am. Chem. Soc.*, **121**, 1922 (1999).
- [77] P.K. Chattaraj, S. Giri. *J. Phys. Chem. A*, **111**, 11116 (2007).
- [78] G. Speier, J. Csihony, A.M. Whalen, C.G. Pierpont. *Inorg. Chem.*, **35**, 3519 (1996).
- [79] S. Sagdinc, B. Köksoy, F. Kandemirli, S.H. Bayari. *J. Mol. Struct.*, **917**, 63 (2009).
- [80] T. Koopmans. *Physica*, **1**, 104 (1934).
- [81] J.I. Aihara. *J. Phys. Chem. A*, **103**, 7487 (1999).
- [82] R.G. Pearson. *Hard and Soft Acids and Bases*, Dowden, Hutchinson and Ross, Stroudsburg, PA (1973).
- [83] R.G. Parr, P.K. Chattaraj. *J. Am. Chem. Soc.*, **113**, 1854 (1991).
- [84] A.A. El-Sherif, M.S. Aljhadali. *Inorg. Chim. Acta*, **407**, 58 (2013).
- [85] I. Sovago, T. Kiss, A. Gergely. *Pure Appl. Chem.*, **65**, 1029 (1993).
- [86] L.D. Pettit. *Pure Appl. Chem.*, **56**, 247 (1984).
- [87] K. Denbigh. *Principles of Chemical Equilibrium*, Cambridge University Press, London (1955).
- [88] A.A. El-Sherif. In *Stoichiometry and Research. The Importance of Quantity in Biomedicine*, A. Innocenti (Ed.), Chap. 4, pp. 79–120, In-Tech Publisher, Rijeka (2012).
- [89] A.E. Martell, R.M. Smith. *Amino Acids, Critical Stability Constants*, Plenum Press, New York (1974).
- [90] J.E. Huheey. *Inorganic Chemistry-Principles of Structure and Reactivity*, Harper SI Edn, New York (1983).
- [91] M. Khan, G. Bouet, F. Vierling, J. Meullemeestre, M.-J. Schwing. *Transition Met. Chem.*, **21**, 231 (1996).
- [92] H.M. Irving, R.J.P. Williams. *J. Chem. Soc.*, 3192 (1953).
- [93] M.T. Beck. *Chemistry of Complex Equilibria.*, Akademiai Kiado, Budapest (1970).
- [94] F.A. Cotton, G. Wilkinson. *Advanced Inorganic Chemistry*, Wiley, London (1962).
- [95] H. Sigel. *Coordination Chemistry*, Vol. 20, Pergamon Press, Oxford (1980).
- [96] K. Maskos. *Acta Biochim. Polonica*, **28**, 183 (1981).
- [97] R.B. Martin, R. Prados. *J. Inorg. Nucl. Chem.*, **36**, 1665 (1974).
- [98] R. DeWitt, J.I. Watters. *J. Am. Chem. Soc.*, **76**, 3810 (1954).
- [99] R.P. Bonomo, S. Musumeci, E. Rizzarelli, S. Sammartano. *Inorg. Chim. Acta*, **14**, 251 (1975).
- [100] C.S.G. Phillips, R.J.P. Williams. *Inorganic Chemistry*, Vol. 2, p. 268, Oxford University Press, Oxford (1966).
- [101] B. Jeragh, D. Al-Wahaib, A.A. El-Sherif, A. El-Dissouky. *J. Chem. Eng. Data*, **52**, 1609 (2007).
- [102] H. Irving, R.J.P. Williams. *Analyst*, **77**, 813 (1952).
- [103] F.R. Harlly, R.M. Burgess, R.M. Alcock. *Solution Equilibria*, p. 257, Ellis Harwood, Chichester (1980).
- [104] A.L. Koch. *Clin. Microbiol. Rev.*, **16**, 673 (2003).
- [105] B.G. Tweedy. *Phytopathology*, **55**, 910 (1964).
- [106] I. Pal, F. Basuli, S. Bhattacharya. *J. Chem. Sci.*, **114**, 255 (2002).
- [107] S. Caglar, E. Adiguzel, B. Sariboga, E. Temel, O. Buyukgungor. *J. Coord. Chem.*, **67**, 670 (2014).
- [108] M.S. Aljhadali, A.T. Abedel Karim, A.A. El-Sherif, M.M. Ahmed. *J. Coord. Chem.*, **67**, 870 (2014).
- [109] H. Liu, Y.-L. Zou, L. Zhang, J.-X. Liu, C.-Y. Song, D.-F. Chai, G.-G. Gao, Y.-F. Qiu. *J. Coord. Chem.*, **67**, 2257 (2014).
- [110] M. Carcelli, P. Mazza, C. Pelizzi, G. Pelizzi, F. Zani. *J. Inorg. Biochem.*, **57**, 43 (1995).
- [111] G.L. Parrilha, J.G. da Silva, L.F. Gouveia, A.K. Gasparoto, R.P. Dias, W.R. Rocha, D.A. Santos, N.L. Speziali, H. Beraldo. *Eur. J. Med. Chem.*, **46**, 1473 (2011).